



Understanding the drivers of marine liquid-water cloud occurrence and properties with global observations using neural networks

Hendrik Andersen¹, Jan Cermak¹, Julia Fuchs¹, Reto Knutti², and Ulrike Lohmann²

¹Karlsruhe Institute of Technology (KIT), Institute of Meteorology and Climate Research, and Institute of Photogrammetry and Remote Sensing

²ETH Zürich, Institute of Atmospheric and Climate Science, Zurich, Switzerland

Correspondence to: Hendrik Andersen (hendrik.andersen@kit.edu)

Abstract. The role of aerosols, clouds and their interactions with radiation remain among the largest unknowns in the climate system. Even though the processes involved are complex, aerosol-cloud interactions are often analyzed by means of bivariate relationships. In this study, 15 years (2001–2015) of monthly satellite-retrieved nearly-global aerosol products are combined with reanalysis data of various meteorological parameters to predict satellite-derived marine liquid-water cloud occurrence and properties by means of regionally-specific artificial neural networks. The statistical models used are shown to be capable of predicting clouds, especially in regions of high cloud variability. At this monthly scale, lower tropospheric stability is shown to be the main determinant of cloud fraction and droplet size, especially in stratocumulus regions, while boundary layer height controls the liquid-water amount and thus the optical thickness of clouds. While aerosols show the expected impact on clouds, at this scale they are less relevant than some meteorological factors. Global patterns of the derived sensitivities point to regional characteristics of aerosol and cloud processes.

1 Motivation and aim

Clouds and their microphysical properties play a central role in the Earth's radiative budget by increasing the albedo but also by interacting with outgoing thermal radiation, leading to a net cooling effect (Boucher et al., 2013). Low-level marine liquid-water clouds are the cloud type with the biggest net cooling effect; their shortwave signal by far exceeds their longwave signal (Hartmann et al., 1992; Wood, 2012; Russell et al., 2013; Chen et al., 2014). A global increase in the occurrence frequency or cooling properties of marine low-level liquid-water clouds could thus offset some of the greenhouse gas warming (Latham et al., 2008). Thus, a complete understanding of the physical processes that determine marine liquid-water clouds and their properties is critical.

Atmospheric aerosols are essential for the formation of clouds, influencing cloud properties as cloud condensation nuclei. An increase in aerosol particles leads to a higher cloud droplet number concentration, and, assuming a constant cloud water content, to smaller droplet radii. This changes the cloud's radiative properties, as the larger overall droplet surface area increases cloud reflectivity (Twomey, 1977). These changes in droplet number concentration and size are also thought to have ramifications on cloud lifetime (Albrecht, 1989) and cloud vertical extent (Pincus and Baker, 1994). However, these processes are nonlinear (Bréon et al., 2002; Koren et al., 2014; Andersen et al., 2016; Glassmeier and Lohmann, 2016) and dependent on various



environmental conditions (e.g. Loeb and Schuster, 2008; Stevens and Feingold, 2009; Su et al., 2010; Andersen and Cermak, 2015; Andersen et al., 2016).

Even though there have been significant efforts and advances in understanding aerosol-cloud interactions (ACI) over the last decades, the overall scientific understanding is still considered as low (Boucher et al., 2013). This springs from the complexity of ACI and cloud processes themselves, the temporal and spatial scales at which these processes occur, as well as challenges in observing them.

In the satellite observational community, a typical investigative approach to analyze ACI is to directly relate aerosol and cloud observations quantitatively using bivariate statistics, often explicitly considering one or two meteorological variables (c.f. e.g. Matsui et al., 2004, 2006; Chen et al., 2014; Andersen and Cermak, 2015). Even though important process inferences have been made on this basis, the limitation of said method set is clearly that the complexity of the processes is not mirrored by the complexity of the statistical method: only selected aspects of the aerosol-cloud system can be analyzed at one time. A multivariate analysis of the relationships between cloud properties and various predictors, including aerosol and meteorological conditions, might be more appropriate for an adequate representation of these atmospheric interactions. In this spirit, this study combines near-global observational and reanalysis data sets as predictors in a multilayer perceptron artificial neural network (ANN) to model near-global marine water cloud occurrence and properties. The main goal of this study is to identify the main drivers of marine liquid-water cloud occurrence as well as physical and optical properties on a global scale, estimate sensitivities for each predictor, and determine regional patterns therein.

The guiding hypotheses are:

1. Neural networks are capable of skillfully modeling cloud patterns on monthly time scales, and allow for a separation and estimates of the relative importance of aerosol and various meteorological factors.
2. Global aerosol and cloud patterns are not only related at a global scale, regional patterns exist.
3. While aerosols are a key determinant for cloud occurrence and properties, other factors are at least equally relevant at the spatial and temporal scales considered here.

2 Data and methods

2.1 Data sets

The analysis uses 15 years (2001–2015) of nearly global (60°N–60°S) satellite retrievals and reanalysis fields. Monthly averages of level 3 collection 6 products based on measurements by the Moderate Resolution Imaging Spectroradiometer (MODIS) sensor on the Terra platform (Levy et al., 2013) are used for information on cloud fraction (CLF; data set: Cloud_Retrieval_Fraction_Liquid_FMean), cloud-top droplet effective radius (CDR; data set: Cloud_Effective_Radius_Liquid_Mean_Mean), cloud liquid water path (LWP; data set: Cloud_Water_Path_37_Liquid_Mean_Mean) and cloud optical thickness (COT; data set: Cloud_Optical_Thickness_Liquid_Mean_Mean). To confine the analysis to liquid-water clouds,



only liquid-water cloud products are used. Information on aerosol loading as a proxy for cloud condensation nuclei is provided by aerosol optical depth at $0.55 \mu\text{m}$ (AOD; data set: Aerosol_Optical_Depth_Land_Ocean_Mean_Mean). Some constraints of AOD are that it can be affected by aerosol swelling due to hydration in humid environments, that it is proportional to aerosol mass and not CCN concentration, and that the retrieval describes vertically integrated information and not specifically aerosol
5 at cloud base height where cloud condensation nuclei are typically activated (Shinozuka et al., 2015). Stier (2016) discusses that in 71 % of the ocean area, AOD only explains 25 % of the cloud condensation nuclei (CCN) variance at cloud base. Still, it is commonly used as a proxy for the columnar aerosol concentration or CCN in ACI studies (Andreae, 2009; Quaas et al., 2009, 2010; Peters et al., 2012; Koren et al., 2012).

Satellite retrievals are combined with reanalysis data sets from the European Centre for Medium-Range Weather Forecasts
10 (ECMWF) for information on meteorological predictors. The ERA-Interim reanalysis provides data for the time since 1979 and is still continued (Dee et al., 2011). Monthly means of mean daily reanalysis data are used for information on various meteorological predictors at selected atmospheric pressure levels. Meteorological determinants may be grouped into information on relative humidity (RH - at pressure levels 950 hPa (Andersen and Cermak, 2015), 850 hPa (Chen et al., 2014) and 700 hPa (Engström and Ekman, 2010)), vertical velocity (W - at pressure levels 950 hPa, 850 hPa (Kaufman et al., 2005; Engström
15 and Ekman, 2010) and 700 hPa (Engström and Ekman, 2010)), boundary layer height (BLH (Painemal et al., 2014)) and lower tropospheric stability (LTS - computed as the difference in potential temperature between 700 hPa and the surface (Klein and Hartmann, 1993; Chen et al., 2014; Andersen and Cermak, 2015; Andersen et al., 2016)). The reanalysis data used features an original spatial resolution of $0.5^\circ \times 0.5^\circ$ and is subsequently resampled to fit the MODIS $1^\circ \times 1^\circ$ grid.

Typically, clouds form when air cools off, increasing RH. Once supersaturation is reached, water vapor can condense on the
20 CCN. Predictors are selected that are thought to capture this very basic concept well: Vertical velocity and relative humidity are selected as indicators of cloud dynamics and stratification at various pressure levels. CCN are represented by AOD, and BLH and LTS describe the large-scale setting. All predictors have been shown to be relevant determinants of liquid-water clouds or their interactions with aerosols in the studies named above. When available, vertically resolved information is preferred to column integrated (e.g. RH at three different pressure levels is preferred to total columnar water vapor), in order to trace
25 processes at various atmospheric levels. While a higher number of reasonable predictors is likely to marginally increase the skill of the ANN, it would increase model complexity and make interpretation more difficult.

By design the data sets applied in this study average over time and space. While on these scales, the causal sequence of cloud processes may not be intact and the processes themselves cannot be observed, their overall ramifications are thought to be represented adequately, in that temporal averaging is intended as a proxy for process relationships.

30 2.2 Artificial neural networks and study design

Basics of artificial neural networks

Machine learning systems consist of a set of numerical operators designed to compute a designated output on given input data. The basic principles, such as the number of numerical links between parameters, are fixed. Artificial neural networks can be described as a branch of machine learning systems. Multilayer perceptrons are a specific type of neural network that are



commonly used in the atmospheric sciences and environmental sciences in general, as they are able to model highly nonlinear functions. This type of ANN consists of several layers of interconnected neurons. In general, the architecture of multilayer perceptron ANNs is variable but a typical ANN may consist of an input layer, at least one hidden layer and an output layer. The information from an input pattern is strictly passed from the input layer via the hidden layer(s) to the output layer that yields the desired output pattern (feed-forward ANN). Multilayer perceptron ANNs are fully connected, i.e. each neuron is connected to every neuron in the neighboring layer(s). All connections between neurons in the ANN are specifically weighted so that the information passed to a neuron is the sum of the weighted outputs from the previous layer (net input). The neuron modifies the information by multiplication with a nonlinear transfer function and passes this information through specific weights to all neurons of the following layer (Gardner and Dorling, 1998).

In general, these types of ANNs learn through training. During the training period a subset of the input and output data sets are fed into the ANN. Using this training data, a learning algorithm adjusts the individual weights of each neuron in the network to minimize the error of the output (e.g. the difference between the modeled and observed outputs). The speed of the learning process is adjusted by a learning rate that determines the step size taken during the iterative learning process. While a high learning rate leads to faster convergence, it may miss a global optimum. An additional momentum term adds a fraction of the previous weight change to the current weight change to assist the optimization algorithm out of local minima (Gardner and Dorling, 1998). After the learning algorithm has reached convergence, the predicted output of the network can be compared to the original output for an estimate of model skill. To ensure that the ANN does not only represent the particular data used in the training (overfitting) and is able to generalize the functional relationships underlying the training data, the model is validated using a second independent subset of the input data. If the ANN is able to generalize the relationships between the data sets, the difference between training and validation errors and the overall error are small. The ANN is tested on a third set of independent data to ensure that the model is not overfit to the validation data.

Design of the study and application of the neural network

The ability of the ANN to predict cloud occurrence, properties and radiative effects is dependent not only on an informed choice of predictors, ANN also require sufficient data that fully represent all cases that the ANN is required to generalize, as ANNs perform well for interpolation but poorly for extrapolation (Gardner and Dorling, 1998). In order to circumvent sampling issues and to enable a direct comparability of results in different regions, the near-global data sets are summarized in 40x20 equal area grid cells by aggregating grid cells at the original spatial resolution of $1^\circ \times 1^\circ$. This leads to an increase from the original 180 data points (15 years, 12 months) for each input/output to between 8,000 and 14,000, depending on the number of $1^\circ \times 1^\circ$ pixels that fall into a specific region. The ANN is only applied in grid cells where a minimum of 2000 valid observations exist. In each equal area, an independent ANN is trained over 500 epochs (i.e. number of times the network iterates over the training data) with 60 % of the data, validated and tested on 20 % of the data each. A simple network topology with one hidden layer consisting of five hidden neurons is applied a) for a more comprehensible model and b) to reduce potential overfitting (Gardner and Dorling, 1998). Multilayer perceptrons with just one hidden layer are frequently used in ecological studies (e.g. Hartmann et al., 2008; Cermak and Knutti, 2009) as they have been shown by several independent studies to be able to approximate any



continuous function (Cybenko, 1989; Funahashi, 1989; Hornik et al., 1989; Kecman and Vojislav, 2001; Olden and Jackson, 2002; Di Noia et al., 2013). A hyperbolic tangent is used as the activation function, the weights are initialized randomly from a uniform distribution between -0.1 and 0.1. Gradient descent (Werbos, 1990; Le et al., 2017) is used as the optimization algorithm, with a learning rate of 0.003 and a momentum of 0.01. In-depth testing was undertaken to adjust the details of the model's settings by comparing model skill for a wide number of model setups as in Hartmann et al. (2016). Once the ANN is trained and able to generalize the relationships between the data sets adequately, sensitivity analyses are conducted. Sensitivities are systematically tested by varying each input variable while holding all other input variables constant, e.g., at their average. In this way the individual contributions of each variable can be analyzed (Olden and Jackson, 2002). A schematic view on the general architecture of the ANN and the training, validation and sensitivity steps is given in Fig. 1.

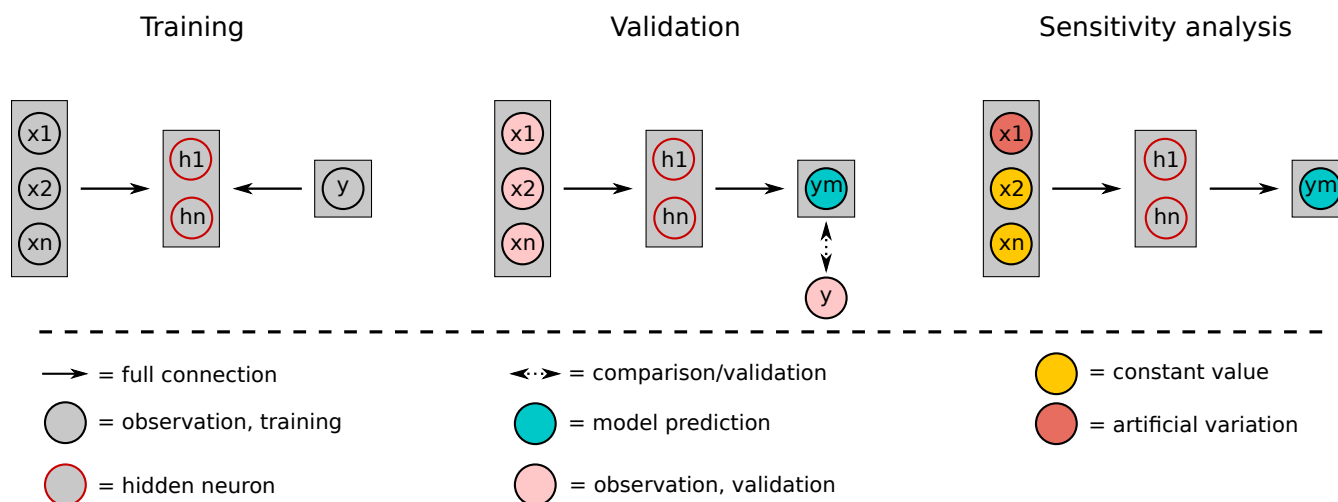


Figure 1. A schematic view on the general architecture and design of multilayer perceptron artificial neural networks. In this study, the ANN features a single hidden layer with 5 neurons.

The ANN skill in modeling the desired outputs is evaluated with the correlation (R^2) between ANN testing output and the corresponding observation data. Sensitivities are only computed for grid cells, where the ANN $R^2 > 0.5$ and the root mean square error relative to the mean (rel. RMSE) $<$ its global average in order to exclude unreasonable models. In order to derive a representative and meaningful sensitivity, the mean of ANN-predicted outputs are compared for two groups of input data: all retrievals of a specific predictor smaller than its 25th percentile and those greater than its 75th percentile; in all cases, the other predictors are held constant at their grid-cell specific mean values. In comparison to a stepwise increase of one specific predictor, a more relevant measure of a typical sensitivity can be derived, as the predictor distribution is considered. Thus, in the context of this study, the sensitivity is defined as the mean difference between the predicted cloud property in the groups of low and high predictor values. Typically, the aerosol effect on e.g. CDR is described by the $\delta \log(CDR) / \delta \log(aerosol)$ relationship, where aerosol can be either AOD or aerosol index (e.g. Costantino and Bréon, 2013). While this gives a regionally comparable estimate of the aerosol-cloud sensitivity, it does not explicitly consider the meteorological framework.



3 Results and discussion

3.1 Skill of the ANN in predicting cloud occurrence and properties

The skill of the ANNs to predict marine liquid-water cloud occurrence, as well as physical and optical properties is shown in Fig. 2 (blue boxes) and contrasted with the skill of a simple correlation between AOD and the cloud properties (red boxes). In the ANN, CLF is predicted with the highest accuracy (mean R^2 of 0.55). While for CDR the skill of the ANN is also > 0.5 for many regions (mean R^2 of 0.45), LWP and COT are predicted less accurately (mean R^2 of 0.35). It is shown that AOD alone typically explains less than 10 % of the cloud property variability.

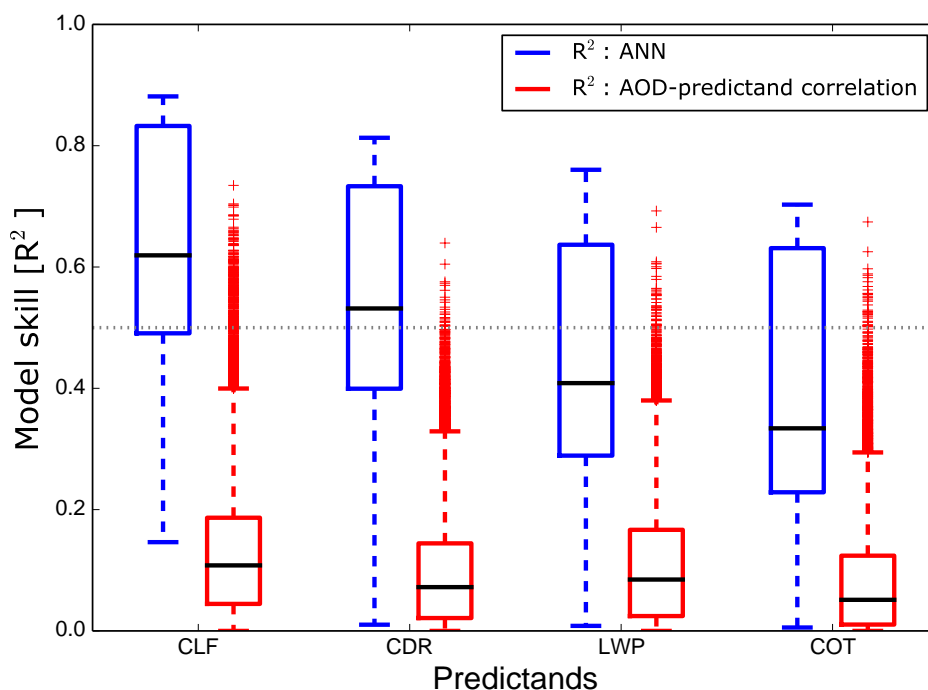


Figure 2. Predictand correlation with ANN (multivariate) test output and AOD (bivariate). The median is represented by the black horizontal line, framed by the interquartile range (boxes), whiskers expand the boxes by 1.5 interquartile ranges.

For all predictands there is a large spread in model skill, leading to distinct regional patterns as illustrated in Fig. 3. The skill of the ANNs is generally higher in the atmospherically stable regions off the western continental coastlines that are dominated by stratocumulus clouds. Less skilled ANNs can generally be found in the (sub-)tropic Pacific and the Indian Ocean.

The global spatial patterns of ANN skill are likely linked to the spatial patterns of the variability of the specific predictands (Fig. 4). A strong dependence on the variability can be noted for CLF and CDR (Fig. 4a and 4b), i.e. a higher variability enables

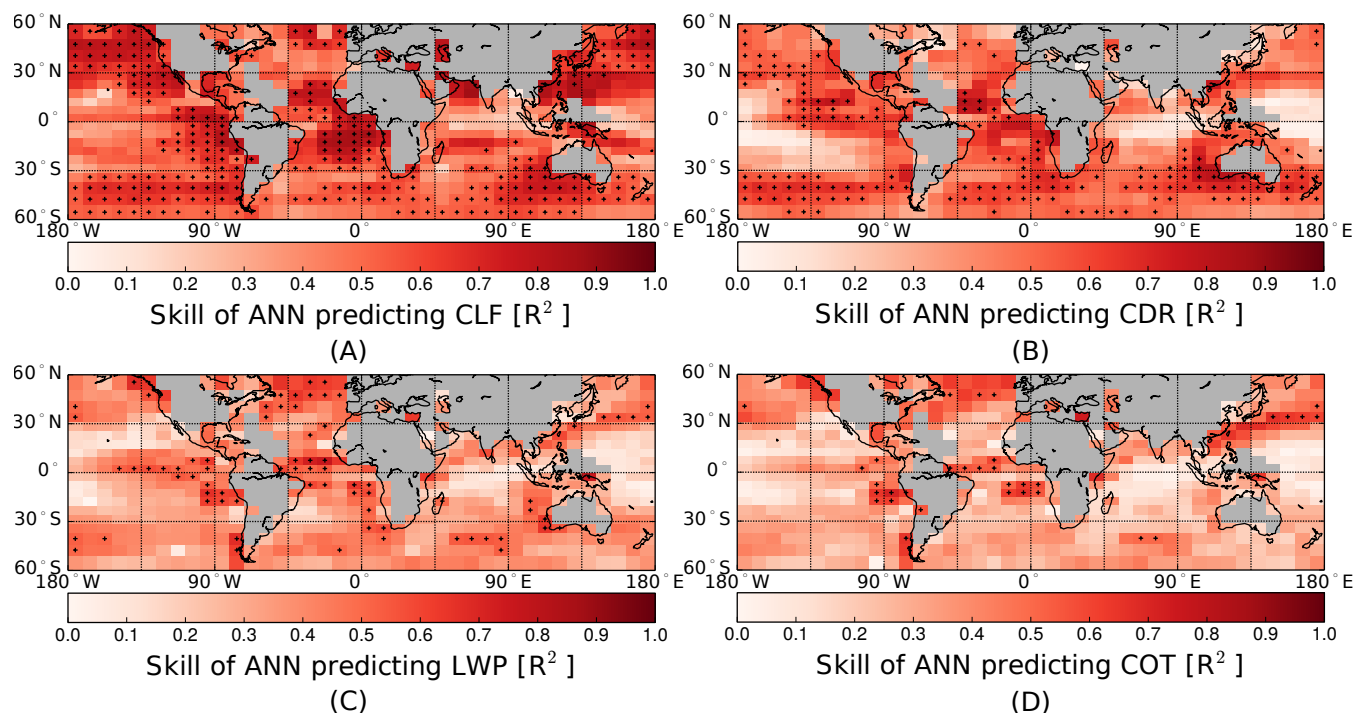


Figure 3. Global patterns of ANN skill [R^2] predicting a) cloud fraction, b) cloud droplet effective radius, c) cloud liquid water path and d) cloud optical thickness. As only ANNs with $R^2 > 0.5$ and rel. RMSE < its global average are used to compute the sensitivities, these are marked by a '+'.

the ANN to more skillfully represent the inherent relationships. This is sensible, as a higher predictand variability offers the ANN a stronger signal from which it can learn.

3.2 Determinants of cloud occurrence and properties

Sensitivities are analyzed in all ANNs with a skill of $R^2 > 0.5$ and with a rel. RMSE that is smaller than its global average.

5 Figure 5 shows globally summarized mean and standard deviation of all predictor sensitivities for CLF (Fig. 5a), CDR (Fig. 5b), LWP (Fig. 5c) and COT (Fig. 5d). Positive sensitivities point towards a positive response to an increase in the specific predictor while holding the other predictors constant at their regional average values. CLF shows the greatest sensitivity to LTS, where an increase in LTS leads to a strong increase in CLF, underlining the importance of LTS found in earlier studies (e.g. Klein and Hartmann, 1993; Matsui et al., 2004; Andersen and Cermak, 2015). CLF is also positively related to relative humidity at all

10 assessed pressure levels, with the strongest sensitivity at 950 hPa, where stratocumulus clouds and transitional clouds between stratocumulus and shallow cumulus are located (Gryspeerd and Stier, 2012; Andersen and Cermak, 2015). While boundary layer height and aerosol are also positively connected to CLF, W sensitivity varies in sign. Sensitivities associated with W can generally be interpreted as the change in the predictand when W changes from updrafts to downdrafts. The most relevant

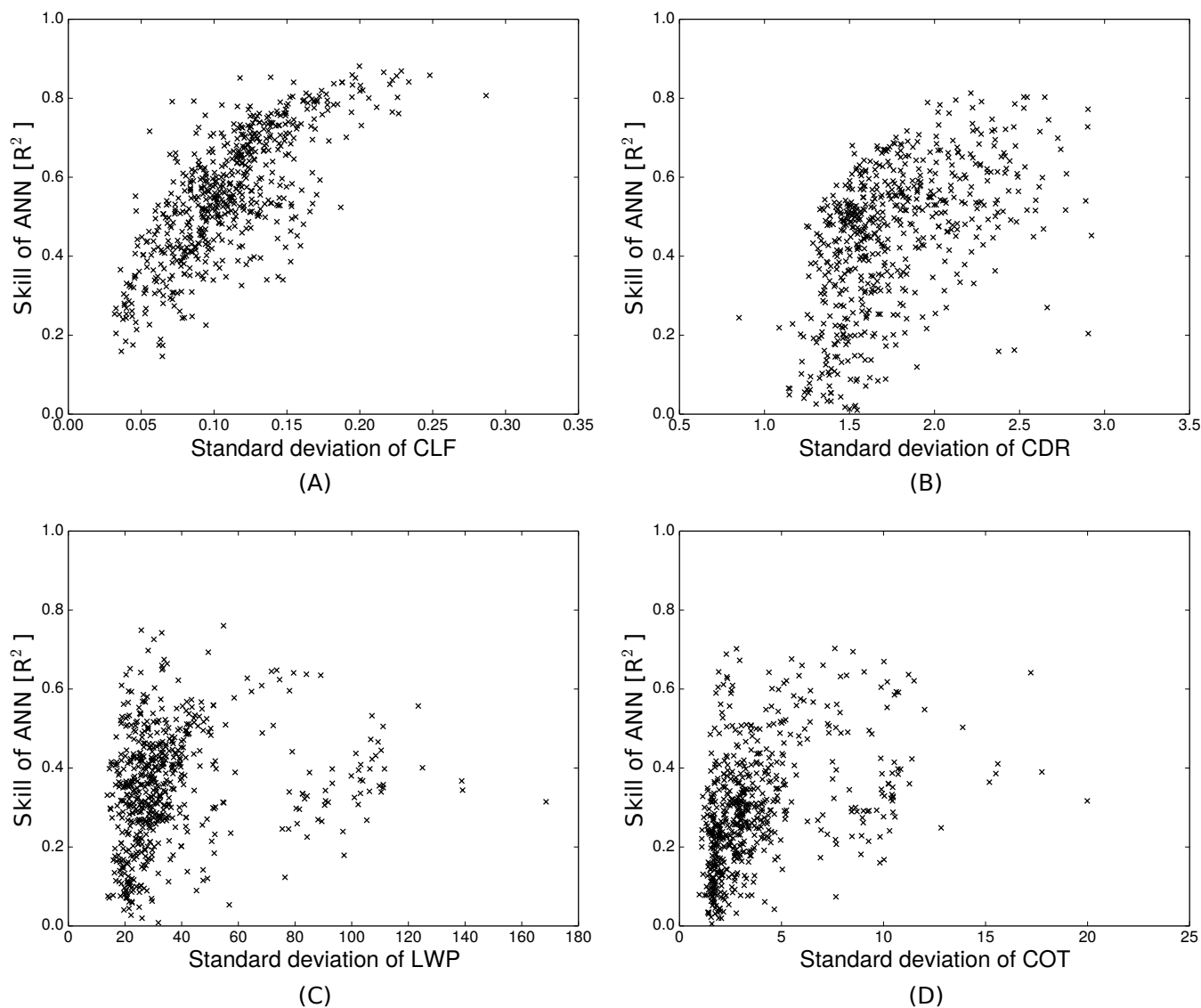


Figure 4. The skill of the ANN predicting a) CLF, b) CDR, c) COT and d) LWP as a function of the predictand variability (standard deviation). Each point illustrates the combination of skill and variability for a specific equal area region.

pressure level in terms of W seems to be 700 hPa, with strong positive sensitivities, illustrating that the downdrafts at 700 hPa associated with stable conditions in the lower troposphere correspond to an increase in CLF. In terms of CDR sensitivities, LTS also displays the strongest effect, with an increase in LTS connected to a distinct reduction in droplet size. RH at 850 hPa exerts the strongest positive CDR sensitivity, with many of the cloud tops located at this pressure level. AOD has a notable sensitivity, showing a distinct negative association to CDR as previously assumed. Generally, updrafts favor larger CDR, with a stronger sensitivity at higher altitudes. Results of LWP and COT sensitivities are similar in terms of the signs and magnitudes of the



individual sensitivities. Both are mainly determined by BLH and LTS, both positively associated with the respective cloud property. RH facilitates thicker clouds containing more liquid water, especially free tropospheric relative humidity at 700 hPa seems to have a positive impact on LWP and COT, as higher humidity levels at 700 hPa are likely to weaken drying effects of entraining air masses (Ackerman et al., 2004; Chen et al., 2012, 2014). While increases in aerosol lead to a negative LWP response, this does not lead to a similarly strong COT reduction. W is negatively related to both cloud properties, as situations with updrafts generally produce thicker clouds, the most relevant pressure level is at 850 hPa.

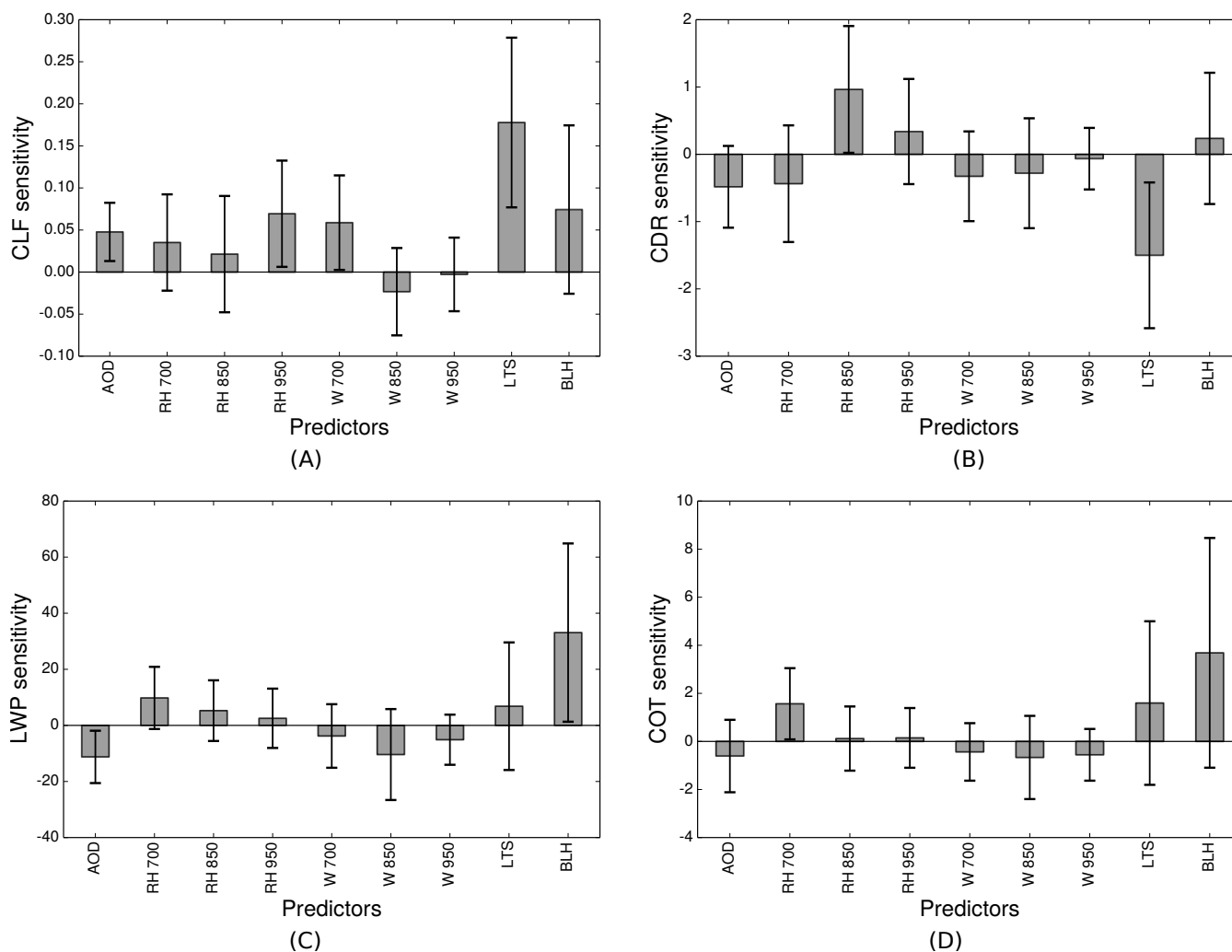


Figure 5. Global mean relative sensitivities as defined in section 2.3 of a) CLF, b) CDR, c) LWP and d) COT for all predictors of the ANNs (x axes). Error bars illustrate the regional variability of the sensitivities (global standard deviation).

The application of an individual ANN in every grid cell enables the analysis of regional patterns of the derived sensitivities. Panels of the left-hand column of Fig. 6 show regional patterns of CLF sensitivities, the panels of the right-hand column show



regional patterns of CDR sensitivities. The range of the colorbars is identical within each column, so that both the overall magnitude as well as the spatial patterns of the sensitivities can be compared. LTS is the strongest determinant for CLF and is positively related to CLF everywhere on Earth, with especially strong sensitivities in atmospherically stable regions off the western coasts of the continents, where stratocumulus clouds are predominant (Klein and Hartmann, 1993; Russell et al., 2013).

5 In these regions RH shows a strong positive CLF sensitivity at 950 hPa, pointing to the relevance of low-level humidity in these regions of low boundary layer clouds. Liquid water cloud fraction in the intertropical convergence zone is more sensitive to RH at 850 hPa, reflecting the thicker boundary layer in this region. The most pronounced relation between the aerosol and CLF can be found at latitudes around 30°, especially over the Northwest Pacific.

CDR is markedly reduced by AOD in the Northwest Pacific and the Southwest Atlantic and negatively associated with AOD
10 to a lesser degree in most other marine regions. The regions over the Northeast Atlantic and close to the coastline of the Arabian Sea are exceptions. In these regions dust particles make up a significant portion of the aerosol species composition (Prospero, 1999; Kaufman et al., 2005), which may lead to larger droplet sizes when dust aerosols act as giant CCN (Levin et al., 2005; Barahona et al., 2010). LTS is negatively associated with CDR, especially south of 30° and in the subtropical Atlantic as found by Matsui et al. (2006), as high LTS environments are connected with weaker updrafts and a shallower boundary layer,
15 limiting cloud droplet growth. This excludes the Southeast Atlantic, where stable conditions may trap the humidity in the boundary layer (Johnson et al., 2004; Painemal et al., 2014; Andersen and Cermak, 2015). Similar effects may occur in the Southeast Pacific as well. RH features the strongest positive CDR sensitivity at 850 hPa with distinctly strong sensitivities in the subtropic regions, where cloud tops are frequently located at this pressure level (Gryspeerd and Stier, 2012). Compared to these factors, W at 700 hPa seems to be a relevant determinant in very selected, mostly tropical regions only.

20 4 Summary and conclusions

The central aim of this study was to identify and analyze the main determinants of marine liquid-water clouds and their sensitivities. Artificial neural networks were shown capable of predicting cloud patterns on a global scale well, although ANN skill is dependent on the cloud property and its variability. Regions with a strong monthly variability such as the stratocumulus regions that feature a strong seasonal cycle are most skillfully represented.

25 Sensitivities were derived for all predictor-predictand combinations, revealing LTS to be the main determinant of monthly liquid-water cloud occurrence and properties. LTS is positively related to CLF on a global scale, with especially strong regional sensitivities in the subsidence regions and the mid-latitudes. In most of these regions, LTS features a strong negative sensitivity towards CDR. One exception to this negative CDR-LTS relationship is the Southeast Atlantic, where high LTS conditions may trap humidity in the boundary layer, causing larger CDR and hence a positive CDR-LTS relationship (Johnson et al., 2004;
30 Painemal et al., 2014; Andersen and Cermak, 2015). The sensitivity of cloud properties to changes in relative humidity is dependent on both region and pressure level. CLF in regions that feature predominantly stratocumulus clouds or other low-level clouds is most sensitive to RH at 950 hPa, whereas tropical regions with thicker boundary layers are more sensitive to RH at higher altitudes. CDR sensitivity to RH is stronger at higher pressure levels, where the cloud-tops are likely located.

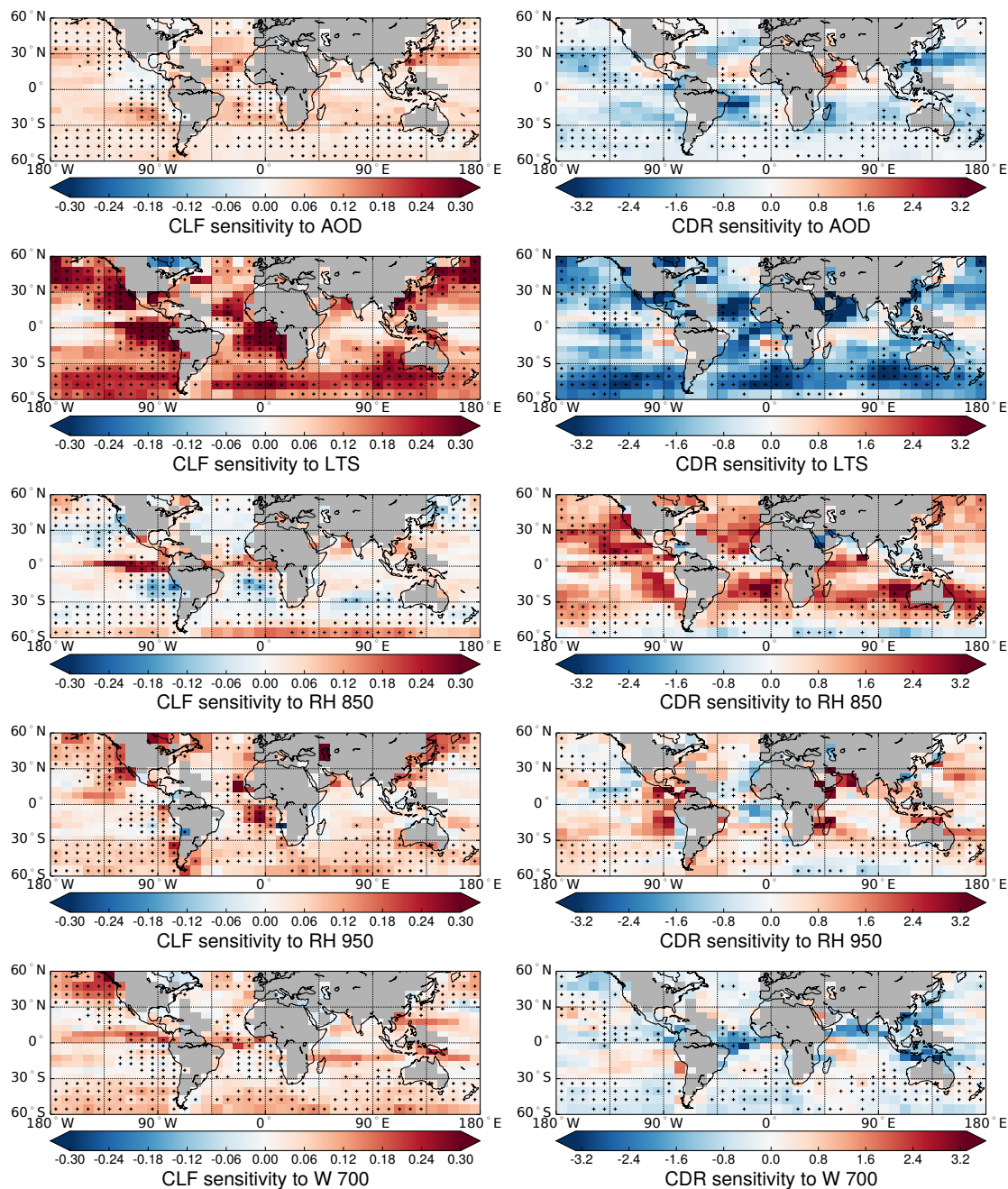


Figure 6. Global relative sensitivity patterns of selected CLF predictors in the left-hand column and CDR predictors in the right-hand column. Gray regions a) are over land or b) do not contain at least 2000 data points. Regions where the ANN test skill (R^2) is > 0.5 and rel. RMSE $<$ its global average are marked with a '+'.



In addition to this, BLH is found to be a main determinant of LWP and COT. One should note though, that not all of the observed predictor-predictand sensitivities are necessarily a result of a direct physical relationship between the predictor and the predictand, but may in part be due to spurious covariations. For example, CLF and AOD are both positively related to RH, potentially contributing to the observed positive AOD-CLF sensitivity. Issues of this kind are addressed here by including information on all relevant parameters in the ANN.

The ramifications of the interactions between aerosols and cloud occurrence and properties seem to be represented well in the ANN, following the general understanding of ACI. Specific regions of interest arise, such as the Northwest Atlantic with strong sensitivities to AOD and regions that are affected by high dust loadings, with positive AOD-CDR relationships and an above average positive AOD-CLF sensitivity.

The results lead to the conclusion that on the system scale the aerosol may be viewed as a relevant determinant of marine liquid-water cloud fraction and microphysical properties, but only a secondary determinant for cloud optical thickness. On the scales considered here, lower tropospheric stability is the key controlling factor of cloud occurrence and droplet size, while boundary layer height controls the liquid water path and thus optical thickness of the cloud. To address climate effects in a straight-forward manner, future research may apply this study's approach to investigate the global determinants of cloud radiative effects.

5 Data availability

MODIS data used in this study were acquired as part of the NASA's Earth-Sun System Division and archived and distributed by the MODIS Adaptive Processing System (MODAPS). MODIS data were obtained from the Goddard Space Flight Center (<http://ladsweb.nascom.nasa.gov/data/search.html>). ECMWF ERA-Interim data used in this study were obtained from the ECMWF data server (<http://apps.ecmwf.int/datasets/data/interim-full-moda/levtype=sfc/>).

Author contributions. J. Cermak had the initial idea and performed a precursor study. H. Andersen fully developed the method and the software, obtained and analyzed the data sets, conducted the original research and wrote the manuscript. H. Andersen, J. Cermak, J. Fuchs, R. Knutti and U. Lohmann contributed to study design and interpretation of findings.

Competing interests. The authors declare that they have no conflict of interest.

Acknowledgements. Funding for this study was provided by Deutsche Forschungsgemeinschaft (DFG) in the project GEOPAC (grant CE 163/5-1).



References

- Ackerman, A. S., Kirkpatrick, M. P., Stevens, D. E., and Toon, O. B.: The impact of humidity above stratiform clouds on indirect aerosol climate forcing, *Nature*, 432, 1014–1017, doi:10.1038/nature03137.1., 2004.
- Albrecht, B. A.: Aerosols, cloud microphysics, and fractional cloudiness, *Science*, 245, 1227–1230, doi:10.1126/science.245.4923.1227, 1989.
- Andersen, H. and Cermak, J.: How thermodynamic environments control stratocumulus microphysics and interactions with aerosols, *Environmental Research Letters*, 10, 24 004, doi:10.1088/1748-9326/10/2/024004, <http://dx.doi.org/10.1088/1748-9326/10/2/024004>, 2015.
- Andersen, H., Cermak, J., Fuchs, J., and Schwarz, K.: Global observations of cloud-sensitive aerosol loadings in low-level marine clouds, *Journal of Geophysical Research: Atmospheres*, 121, 12 936–12 946, doi:10.1002/2016JD025614, <http://doi.wiley.com/10.1002/2016JD025614>, 2016.
- Andreae, M. O.: Correlation between cloud condensation nuclei concentration and aerosol optical thickness in remote and polluted regions, *Atmospheric Chemistry and Physics*, 9, 543–556, doi:10.5194/acp-9-543-2009, 2009.
- Barahona, D., West, R. E. L., Stier, P., Romakkaniemi, S., Kokkola, H., and Nenes, A.: Comprehensively accounting for the effect of giant CCN in cloud activation parameterizations, *Atmospheric Chemistry and Physics*, 10, 2467–2473, 2010.
- Boucher, O., Randall, D., Artaxo, P., Bretherton, C., Feingold, G., Forster, P., Kerminen, V.-M., Kondo, Y., Liao, H., Lohmann, U., Rasch, P., Satheesh, S. K., Sherwood, S., Stevens, B., and Zhang, X.-Y.: Clouds and Aerosols, in: *Climate Change 2013: The Physical Science Basis, Contribution of Working Group I to the Fourth Assessment Report of the Intergovernmental Panel on Climate Change*, [Stocker, T.F., Qin, D., Plattner, G.K., Tignor, M., Allen, S.K., Boschung, J., Nauels, A., Xia, Y., Bex, V. and Midgley, P.M. (eds.)]. Cambridge University Press, Cambridge, United Kingdom and New York, NY, USA., 2013.
- Bréon, F.-M., Tanré, D., and Generoso, S.: Aerosol effect on cloud droplet size monitored from satellite, *Science*, 295, 834–838, doi:10.1126/science.1066434, <http://www.ncbi.nlm.nih.gov/pubmed/11823636>, 2002.
- Cermak, J. and Knutti, R.: Beijing Olympics as an Aerosol Field Experiment, *Geophysical Research Letters*, 36, L10 806, doi:10.1029/2009GL038572, <http://www.iac.ethz.ch/people/knuttir/papers/cermak09grl.pdf>, 2009.
- Chen, Y.-C., Christensen, M. W., Xue, L., Sorooshian, A., Stephens, G. L., Rasmussen, R. M., and Seinfeld, J. H.: Occurrence of lower cloud albedo in ship tracks, *Atmospheric Chemistry and Physics*, 12, 8223–8235, doi:10.5194/acp-12-8223-2012, <http://www.atmos-chem-phys.net/12/8223/2012/>, 2012.
- Chen, Y.-C., Christensen, M. W., Stephens, G. L., and Seinfeld, J. H.: Satellite-based estimate of global aerosol-cloud radiative forcing by marine warm clouds, *Nature Geoscience*, 7, 643–646, doi:10.1038/ngeo2214, 2014.
- Costantino, L. and Bréon, F.-M.: Aerosol indirect effect on warm clouds over South-East Atlantic, from co-located MODIS and CALIPSO observations, *Atmospheric Chemistry and Physics*, 13, 69–88, doi:10.5194/acp-13-69-2013, <http://www.atmos-chem-phys.net/13/69/2013/>, 2013.
- Cybenko, G.: Approximation by superpositions of a sigmoidal function, *Mathematics of Control, Signals, and Systems*, 2, 303–314, doi:10.1007/BF02551274, <http://link.springer.com/10.1007/BF02551274>, 1989.
- Dee, D. P., Uppala, S. M., Simmons, A. J., Berrisford, P., Poli, P., Kobayashi, S., Andrae, U., Balmaseda, M. A., Balsamo, G., Bauer, P., Bechtold, P., Beljaars, A. C. M., van de Berg, L., Bidlot, J., Bormann, N., Delsol, C., Dragani, R., Fuentes, M., Geer, A. J., Haimberger, L., Healy, S. B., Hersbach, H., Hólm, E. V., Isaksen, I., Kållberg, P., Köhler, M., Matricardi, M., McNally, A. P., Monge-Sanz, B. M., Morcrette, J.-J., Park, B.-K., Peubey, C., de Rosnay, P., Tavolato, C., Thépaut, J.-N., and Vitart, F.: The ERA-Interim reanalysis:



- configuration and performance of the data assimilation system, *Quarterly Journal of the Royal Meteorological Society*, 137, 553–597, doi:10.1002/qj.828, <http://doi.wiley.com/10.1002/qj.828>, 2011.
- Di Noia, A., Sellitto, P., Frate, F. D., and De Laat, J.: Global tropospheric ozone column retrievals from OMI data by means of neural networks, *Atmospheric Measurement Techniques*, 6, 895–915, doi:10.5194/amt-6-895-2013, www.atmos-meas-tech.net/6/895/2013/, 2013.
- 5 Engström, A. and Ekman, A. M. L.: Impact of meteorological factors on the correlation between aerosol optical depth and cloud fraction, *Geophysical Research Letters*, 37, L18 814, doi:10.1029/2010GL044361, <http://doi.wiley.com/10.1029/2010GL044361>, 2010.
- Funahashi, K.-I.: On the approximate realization of continuous mappings by neural networks, *Neural Networks*, 2, 183–192, doi:10.1016/0893-6080(89)90003-8, <http://linkinghub.elsevier.com/retrieve/pii/0893608089900038>, 1989.
- Gardner, M. and Dorling, S.: Artificial neural networks (the multilayer perceptron) – a review of applications in the atmospheric sciences, 10 *Atmospheric Environment*, 32, 2627–2636, doi:10.1016/S1352-2310(97)00447-0, 1998.
- Glassmeier, F. and Lohmann, U.: Constraining precipitation susceptibility of warm, ice- and mixed-phase clouds with microphysical equations, *Journal of the Atmospheric Sciences*, 73, 5003–5023, doi:10.1175/JAS-D-16-0008.1, <http://journals.ametsoc.org/doi/10.1175/JAS-D-16-0008.1>, 2016.
- Gryspeerd, E. and Stier, P.: Regime-based analysis of aerosol-cloud interactions, *Geophysical Research Letters*, 39, L21 802, 15 doi:10.1029/2012GL053221, <http://doi.wiley.com/10.1029/2012GL053221>, 2012.
- Hartmann, D. L., Ockert-Bell, M. E., and Michelsen, M. L.: The Effect of Cloud Type on Earth's Energy Balance: Global Analysis, *Journal of Climate*, 5, 1281–1304, doi:10.1175/1520-0442(1992)005<1281:TEOCTO>2.0.CO;2, 1992.
- Hartmann, H., Becker, S., King, L., and Jiang, T.: Forecasting water levels at the Yangtze River with neural networks, *Erdkunde*, 62, 231–243, doi:10.3112/erdkunde.2008.03.04, 2008.
- 20 Hartmann, H., Snow, J. A., Su, B., and Jiang, T.: Seasonal predictions of precipitation in the Aksu-Tarim River basin for improved water resources management, *Global and Planetary Change*, 147, 86–96, doi:10.1016/j.gloplacha.2016.10.018, 2016.
- Hornik, K., Stinchcombe, M., and White, H.: Multilayer feedforward networks are universal approximators, *Neural Networks*, 2, 359–366, doi:10.1016/0893-6080(89)90020-8, <http://linkinghub.elsevier.com/retrieve/pii/0893608089900208>, 1989.
- Johnson, B., Shine, K., and Forster, P.: The semi-direct aerosol effect: Impact of absorbing aerosols on marine stratocumulus, *Quarterly Journal of the Royal Meteorological Society*, 130, 1407–1422, doi:10.1256/qj.03.61, <http://doi.wiley.com/10.1256/qj.03.61>, 2004.
- 25 Kaufman, Y. J., Koren, I., Remer, L., Rosenfeld, D., and Rudich, Y.: The effect of smoke, dust, and pollution aerosol on shallow cloud development over the Atlantic Ocean, *Proceedings of the National Academy of Sciences of the United States of America*, 102, 11 207–11 212, doi:10.1073/pnas.0505191102, <http://www.pubmedcentral.nih.gov/articlerender.fcgi?artid=1182178&tool=pmcentrez&rendertype=abstract>, 2005.
- 30 Kecman, V. V. and Vojislav: *Learning and soft computing: support vector machines, neural networks, and fuzzy logic models*, MIT Press, <http://dl.acm.org/citation.cfm?id=559026>, 2001.
- Klein, S. A. and Hartmann, D. L.: The Seasonal Cycle of Low Stratiform Clouds, *Journal of Climate*, 6, 1587–1606, doi:10.1175/1520-0442(1993)006<1587:TSCOLS>2.0.CO;2, 1993.
- Koren, I., Altaratz, O., Remer, L. A., Feingold, G., Martins, J. V., and Heiblum, R. H.: Aerosol-induced intensification of rain from the tropics 35 to the mid-latitudes, *Nature Geoscience*, 5, 118–122, doi:10.1038/ngeo1364, <http://www.nature.com/doi/10.1038/ngeo1364>, 2012.
- Koren, I., Dagan, G., and Altaratz, O.: From aerosol-limited to invigoration of warm convective clouds, *Science*, 344, 1143–1146, doi:10.1126/science.1252595, <http://www.sciencemag.org/content/344/6188/1143.full>, 2014.



- Latham, J., Rasch, P., Chen, C.-C., Kettles, L., Gadian, A., Gettelman, A., Morrison, H., Bower, K., and Choulaton, T.: Global temperature stabilization via controlled albedo enhancement of low-level maritime clouds, *Philosophical Transactions of the Royal Society of London A: Mathematical, Physical and Engineering Sciences*, 366, 3969–3987, doi:10.1098/rsta.2008.0137, file:///Users/yangyang/YANGYANGXU/work/lynn[_]research/papersfromlynn/Lathametal.-2008-Philosophicaltransactions.SeriesA,
- 5 Mathematical, physical, and engineering sciences-Global temperature stabilization via controlled albedo enhancement of flow, 2008.
- Le, J., El-Askary, H., Allali, M., and Struppa, D.: Application of recurrent neural networks for drought projections in California, *Atmospheric Research*, 188, 100–106, doi:10.1016/j.atmosres.2017.01.002, <http://linkinghub.elsevier.com/retrieve/pii/S0169809517300157>, 2017.
- Levin, Z., Teller, A., Ganor, E., and Yin, Y.: On the interactions of mineral dust, sea-salt particles, and clouds: A measurement and modeling study from the Mediterranean Israeli Dust Experiment campaign, *Journal of Geophysical Research: Atmospheres*, 110, 1–19,
- 10 doi:10.1029/2005JD005810, 2005.
- Levy, R. C., Mattoo, S., Munchak, L. A., Remer, L. A., Sayer, A. M., Patadia, F., and Hsu, N. C.: The Collection 6 MODIS aerosol products over land and ocean, *Atmospheric Measurement Techniques*, 6, 2989–3034, doi:10.5194/amt-6-2989-2013, <http://www.atmos-meas-tech.net/6/2989/2013/amt-6-2989-2013.html>, 2013.
- Loeb, N. G. and Schuster, G. L.: An observational study of the relationship between cloud, aerosol and meteorology in broken low-level cloud conditions, *Journal of Geophysical Research: Atmospheres*, 113, D14 214, doi:10.1029/2007JD009763, <http://doi.wiley.com/10.1029/2007JD009763>, 2008.
- Matsui, T., Masunaga, H., and Pielke Sr., R. A.: Impact of aerosols and atmospheric thermodynamics on cloud properties within the climate system, *Geophysical Research Letters*, 31, L06 109, doi:10.1029/2003GL019287, <http://doi.wiley.com/10.1029/2003GL019287>, 2004.
- Matsui, T., Masunaga, H., Kreidenweis, S. M., Pielke, R. A., Tao, W.-K., Chin, M., and Kaufman, Y. J.: Satellite-based assessment of marine
- 20 low cloud variability associated with aerosol, atmospheric stability, and the diurnal cycle, *Journal of Geophysical Research: Atmospheres*, 111, D17 204, doi:10.1029/2005JD006097, <http://doi.wiley.com/10.1029/2005JD006097>, 2006.
- Olden, J. D. and Jackson, D. A.: Illuminating the "black box": A randomization approach for understanding variable contributions in artificial neural networks, *Ecological Modelling*, 154, 135–150, doi:10.1016/S0304-3800(02)00064-9, 2002.
- Painemal, D., Kato, S., and Minnis, P.: Boundary layer regulation in the southeast Atlantic cloud microphysics during the biomass
- 25 burning season as seen by the A-train satellite constellation, *Journal of Geophysical Research: Atmospheres*, 119, 11 288–11 302, doi:10.1002/2014JD022182, <http://doi.wiley.com/10.1002/2014JD022182>, 2014.
- Peters, K., Stier, P., Quaas, J., and Graßl, H.: Aerosol indirect effects from shipping emissions: sensitivity studies with the global aerosol-climate model ECHAM-HAM, *Atmospheric Chemistry and Physics*, 12, 5985–6007, doi:10.5194/acp-12-5985-2012, <http://www.atmos-chem-phys.net/12/5985/2012/>, 2012.
- 30 Pincus, R. and Baker, M. B.: Effect of precipitation on the albedo susceptibility of clouds in the marine boundary layer, *Nature*, 372, 250–252, doi:10.1038/372250a0, 1994.
- Prospero, J. M.: Long-range transport of mineral dust in the global atmosphere: impact of African dust on the environment of the southeastern United States, *Proceedings of the National Academy of Sciences of the United States of America*, 96, 3396–403, doi:10.1073/PNAS.96.7.3396, <http://www.ncbi.nlm.nih.gov/pubmed/10097049> <http://www.pubmedcentral.nih.gov/articlerender.fcgi?artid=PMC34280>, 1999.
- 35 Quaas, J., Ming, Y., Menon, S., Takemura, T., Wang, M., Penner, J. E., Gettelman, A., Lohmann, U., Bellouin, N., Boucher, O., Sayer, A. M., Thomas, G. E., McComiskey, A., Feingold, G., Hoose, C., Kristjánsson, J. E., Liu, X., Balkanski, Y., Donner, L. J., Ginoux, P. A., Stier, P., Feichter, J., Sednev, I., Bauer, S. E., Koch, D., Grainger, R. G., Kirkevåg, A., Iversen, T., Seland, Ø., Easter, R., Ghan, S. J., Rasch, P. J.,



- Morrison, H., Lamarque, J., Iacono, M. J., Kinne, S., and Schulz, M.: Aerosol indirect effects - general circulation model intercomparison and evaluation with satellite data, *Atmospheric Chemistry and Physics*, 9, 8697–8717, doi:10.5194/acp-9-8697-2009, 2009.
- Quaas, J., Stevens, B., Stier, P., and Lohmann, U.: Interpreting the cloud cover - aerosol optical depth relationship found in satellite data using a general circulation model, *Atmospheric Chemistry and Physics*, 10, 6129–6135, <http://www.atmos-chem-phys.net/10/6129/2010/>, 2010.
- 5 Russell, L. M., Sorooshian, A., Seinfeld, J. H., Albrecht, B. A., Nenes, A., Ahlm, L., Chen, Y.-C., Coggon, M., Craven, J. S., Flagan, R. C., Frossard, A. A., Jonsson, H., Jung, E., Lin, J. J., Metcalf, A. R., Modini, R., Mülmenstädt, J., Roberts, G., Shingler, T., Song, S., Wang, Z., and Wonaschütz, A.: Eastern Pacific Emitted Aerosol Cloud Experiment, *Bulletin of the American Meteorological Society*, 94, 709–729, doi:10.1175/BAMS-D-12-00015.1, <http://journals.ametsoc.org/doi/abs/10.1175/BAMS-D-12-00015.1>, 2013.
- Shinozuka, Y., Clarke, A. D., Nenes, A., Jefferson, A., Wood, R., McNaughton, C. S., Ström, J., Tunved, P., Redemann, J., Thornhill, K. L.,
10 Moore, R. H., Latham, T. L., Lin, J. J., and Yoon, Y. J.: The relationship between cloud condensation nuclei (CCN) concentration and light extinction of dried particles: indications of underlying aerosol processes and implications for satellite-based CCN estimates, *Atmospheric Chemistry and Physics*, 15, 7585–7604, doi:10.5194/acp-15-7585-2015, <http://www.atmos-chem-phys.net/15/7585/2015/>, 2015.
- Stevens, B. and Feingold, G.: Untangling aerosol effects on clouds and precipitation in a buffered system, *Nature*, 461, 607–613, doi:10.1038/nature08281, <http://www.ncbi.nlm.nih.gov/pubmed/19794487>, 2009.
- 15 Stier, P.: Limitations of passive remote sensing to constrain global cloud condensation nuclei, *Atmospheric Chemistry and Physics*, 16, 6595–6607, doi:10.5194/acp-16-6595-2016, <http://www.atmos-chem-phys.net/16/6595/2016/>, 2016.
- Su, W., Loeb, N. G., Xu, K.-M., Schuster, G. L., and Eitzen, Z. A.: An estimate of aerosol indirect effect from satellite measurements with concurrent meteorological analysis, *Journal of Geophysical Research: Atmospheres*, 115, D18 219, doi:10.1029/2010JD013948, 2010.
- Twomey, S.: The Influence of Pollution on the Shortwave Albedo of Clouds, *Journal of the Atmospheric Sciences*, 34, 1149–1152,
20 doi:10.1175/1520-0469(1977)034<1149:TIOPOT>2.0.CO;2, 1977.
- Werbos, P.: Backpropagation through time: what it does and how to do it, *Proceedings of the IEEE*, 78, 1550–1560, doi:10.1109/5.58337, <http://ieeexplore.ieee.org/document/58337/>, 1990.
- Wood, R.: Stratocumulus Clouds, *Monthly Weather Review*, 140, 2373–2423, doi:10.1175/MWR-D-11-00121.1, 2012.